

AD-A190 391

INFRARED-SENSITIVE SPATIAL LIGHT MODULATOR(U)
MASSACHUSETTS INST OF TECH CAMBRIDGE DEPT OF ELECTRICAL
ENGINEERING AND COMPU TER SCIENCE C HARDE NOV 87

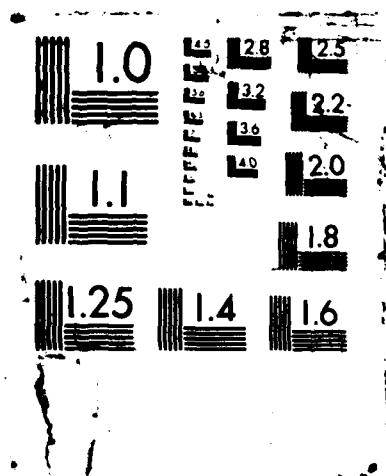
1/1

UNCLASSIFIED

AFATL-TR-87-32 F08635-84-K-0209

F/G 17/5.1 NL





AFATL-TR-87-32

DTIC FILE COPY

Infrared-Sensitive Spatial Light Modulator

AD-A190 391

Cardinal Warde

DEPARTMENT OF ELECTRICAL ENGINEERING
AND COMPUTER SCIENCE
MASSACHUSETTS INSTITUTE OF TECHNOLOGY
CAMBRIDGE, MASSACHUSETTS 02139

NOVEMBER 1987

DTIC
ELECTE
JAN 12 1988
S D

FINAL REPORT FOR PERIOD JUNE 1984-MAY 1987

APPROVED FOR PUBLIC RELEASE; DISTRIBUTION UNLIMITED

AIR FORCE ARMAMENT LABORATORY
Air Force Systems Command ■ United States Air Force ■ Eglin Air Force Base, Florida

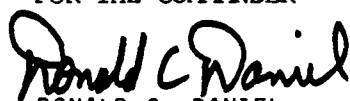
NOTICE

When Government drawings, specifications, or other data are used for any purpose other than in connection with a definitely Government-related procurement, the United States Government incurs no responsibility nor any obligation whatsoever. The fact that the Government may have formulated or in any way supplied the said drawings, specifications, or other data, is not to be regarded by implication, or otherwise as in any manner construed, as licensing the holder, or any other person or corporation; or conveying any rights or permission to manufacture, use, or sell any patented invention that may in any way be related thereto.

The AFATL STINFO Officer has reviewed this report, and it is releasable to the National Technical Information Service (NTIS), where it will be available to the general public, including foreign nationals.

This report has been reviewed and is approved for publication.

FOR THE COMMANDER



DONALD C. DANIEL

Chief, Advanced Guidance Division

Even though this report may contain special release rights held by the controlling office, please do not request copies from the Air Force Armament Laboratory. If you qualify as a recipient, release approval will be obtained from the originating activity by DTIC. Address your request for additional copies to:

Defense Technical Information Center
Cameron Station
Alexandria, VA 22304-6145

If your address has changed, if you wish to be removed from our mailing list, or if your organization no longer employs the addressee, please notify AFATL/AGS, Eglin AFB, FL 32542-5434, to help us maintain a current mailing list.

Copies of this report should not be returned unless return is required by security considerations, contractual obligations, or notice on a specific document.

Unclassified

SECURITY CLASSIFICATION OF THIS PAGE

AD-A190391

REPORT DOCUMENTATION PAGE

1a. REPORT SECURITY CLASSIFICATION Unclassified			1b. RESTRICTIVE MARKINGS		
2a. SECURITY CLASSIFICATION AUTHORITY			3. DISTRIBUTION / AVAILABILITY OF REPORT Approved for public release; distribution unlimited		
2b. DECLASSIFICATION / DOWNGRADING SCHEDULE					
4. PERFORMING ORGANIZATION REPORT NUMBER(S)			5. MONITORING ORGANIZATION REPORT NUMBER(S) AFATL-TR-87-32		
6a. NAME OF PERFORMING ORGANIZATION Massachusetts Institute of Technology		6b. OFFICE SYMBOL (if applicable)	7a. NAME OF MONITORING ORGANIZATION Air-to-Surface Guidance Branch Advanced Guidance Division		
6c. ADDRESS (City, State, and ZIP Code) Department of Electrical Engineering and Computer Science Cambridge, Massachusetts 02139			7b. ADDRESS (City, State, and ZIP Code) Air Force Armament Laboratory Elgin Air Force Base, FL 32542-5000		
8a. NAME OF FUNDING / SPONSORING ORGANIZATION Advanced Guidance Division		8b. OFFICE SYMBOL (if applicable) AFATL/AGS	9. PROCUREMENT INSTRUMENT IDENTIFICATION NUMBER F08635-84-K-0209		
8c. ADDRESS (City, State, and ZIP Code) Air Force Armament Laboratory Elgin Air Force Base FL 32542-5434			10. SOURCE OF FUNDING NUMBERS		
			PROGRAM ELEMENT NO. 61101 F	PROJECT NO. 2305	TASK NO. E2
11. TITLE (Include Security Classification) Infrared-Sensitive Spatial Light Modulator					
12. PERSONAL AUTHOR(S) Cardinal Warde					
13a. TYPE OF REPORT Final		13b. TIME COVERED FROM June 84 TO 20 May 87		14. DATE OF REPORT (Year, Month, Day) November 1987	
15. PAGE COUNT 34					
16. SUPPLEMENTARY NOTATION Availability of report specified on Verso of front cover					
17. COSATI CODES			18. SUBJECT TERMS (Continue on reverse if necessary and identify by block number) Spatial light modulator, IR processing device, optical processing component		
FIELD	GROUP	SUB-GROUP			
17	05	01			
14	03				
19. ABSTRACT (Continue on reverse if necessary and identify by block number) This final report summarizes a preliminary investigation of an infrared-sensitive spatial light modulator that is designed to respond to write light in the 3 to 5 μ m wavelength range. The device can be read out with visible light and, as such, is intended to function simultaneously as an image wavelength upconverter and light modulator. The device design employs a thin-film InSb photoconductor that addresses a DKDP crystal which is cooled near the Curie temperature (-51°C) of DKDP. Preliminary results are reported on: thin flash-evaporated films of InSb; the development of the cooled DKDP substrates; design and fabrication of the modulator vacuum cell; theoretical modelling of the device performance.					
20. DISTRIBUTION / AVAILABILITY OF ABSTRACT <input type="checkbox"/> UNCLASSIFIED/UNLIMITED <input checked="" type="checkbox"/> SAME AS RPT. <input type="checkbox"/> DTIC USERS			21. ABSTRACT SECURITY CLASSIFICATION Unclassified		
22a. NAME OF RESPONSIBLE INDIVIDUAL James M. Kirkpatrick			22b. TELEPHONE (Include Area Code) 904-882-2838		22c. OFFICE SYMBOL AFATL/AGS

PREFACE

This program was conducted by the Massachusetts Institute of Technology, Department of Electrical Engineering and Computer Science, Cambridge, Massachusetts 02139, under Contract FO8635-84-K-0209 with the Air Force Armament Laboratory, Eglin Air Force Base, Florida 32542-5000. James M. Kirkpatrick, AGS, managed the program for the Air Force Armament Laboratory. The program was conducted during the period 1 June, 1984 to 20 May 1987.



Accession For	
NTIS GRA&I	<input checked="" type="checkbox"/>
DTIC TAB	<input type="checkbox"/>
Unannounced	<input type="checkbox"/>
Justification	
By	
Distribution	
Availability Codes	
Dist	Avail and/or Special
A-1	

TABLE OF CONTENTS

Section	Title	Page
I	INTRODUCTION.....	1
	Program goals	1
	Background.....	1
II	APPROACH	2
	Device Design	2
III	PRINCIPLES OF OPERATION OF THE DEVICE.....	4
IV	ELECTRO-OPTIC MATERIALS CONSIDERATIONS.....	6
	Electro-optic Effect in DKDP	6
V	PHOTOCONDUCTOR MATERIALS CONSIDERATIONS.....	8
	Physical Properties of Indium Antimonide (InSb)	8
	Photoconductive Properties of InSb	10
	Noise Considerations	14
	Flash Evaporation	17
	Characterizing Photoconductivity Response of InSb	19
VI	CONCLUSION.....	22
	REFERENCES	23

LIST OF FIGURES

Figure	Title	Page
1a	Architecture of the InSb/DKDP Infrared-Sensitive Light Modulator	2
1b	Photograph of Vacuum-Demountable InSb/DKDP Modulator Cell	3
2	Electrical Model of the Device	4
3	Cubic Unit Cell of the Zinc-Blende Structure Containing Eight Atoms	8
4	Temperature Dependence of Electron and Hole Mobility in InSb (Reference 11)	10
5	Temperature Dependence of Minority and Majority Carrier Lifetimes for P-Type InSb (Reference 11)	11
6	Photoconductivity of a Thin Flash Evaporated Film of InSb	12
7	Typical Spectral Detectivity Range for Cooled Photoconductive InSb of Various Areas; 2π FOV; 77° K, 300° K Background	12
8a	Setup for Flash Evaporation of InSb	18
8b	Actual Flash Evaporation System Used	18
9	Experimental Setup for Measuring Photoconductivity of InSb Films	19
10a	Spectral Output of the Oriel Infrared Lamp Used (Oriel Catalog)	20
10b	Spectral Transmittance of the Germanium Lens (Laser Focus Buyers Guide)	20

LIST OF TABLES

Table	Title	Page
1	Physical Properties of InSb	9
2	Melting Points of III-V Compounds.	9
3	Properties of III-V Compounds at Room Temperature.	9

SECTION I

INTRODUCTION

PROGRAM GOALS

The goals of the program were to design, model, and develop an infrared-sensitive spatial light modulator that would respond in the 3 to 5 μm wavelength range and that would simultaneously perform wavelength image upconversion from the infrared to the visible. The modulator was also expected to have high sensitivity ($\sim 1 \mu\text{J}/\text{cm}^2$), high spatial resolution (~ 10 cycles/mm) and high framing speed (100Hz).

BACKGROUND

For low-light-level, night-vision, and infrared image processing, there is an urgent need for an infrared-sensitive spatial light modulator that can be read out at visible wavelengths. Such a modulator with high sensitivity would find immediate applications in scenarios where it is necessary to simultaneously perform wavelength upconversion with gain, and incoherent to coherent conversion for real-time signal processing.

Of the commercially available optically addressed spatial light modulators, the PROM (Reference 1), and LCLV (Reference 2), are not sensitive to write light with wavelength beyond the red portion of the visible spectrum, and the conventional microchannel spatial light modulator (MLSM) (Reference 3-5) with a cesiated gallium arsenide photocathode will not respond beyond 1.2 μm wavelength. The Soviets have also been concerned with this problem and have constructed a GaAs/liquid crystal light valve for near infrared to visible conversion (Reference 6). They have shown that semiconductor/insulator spatial light modulators can have extremely high halfwave exposure sensitivity in the 10^{-8} to 10^{-9} J/cm^2 range (Reference 7).

SECTION II

APPROACH

The technology that was investigated in this research program involved the fabrication of a sandwich structure of an infrared-sensitive photoconductor (InSb) and a DKDP electro-optic crystal wafer cooled near the Curie temperature of DKDP (-51°C). Operating the modulator at low temperature does not present any extra inconvenience since the semiconductor detector layer should be cooled for optimum operation. The low temperature precludes the use of liquid crystals in the electro-optic layer.

DEVICE DESIGN

The architecture of the device is illustrated in Figure 1a. The electro-optic DKDP crystal is coated on the readout side with a transparent (visible) electrode and, on the other side, with a dielectric mirror/light blocking layer. The infrared detector structure is a matrix of independent InSb detector pixels that is biased with a common electrode on one side and bonded to the dielectric mirror/light-blocking layer on the other. This multi-layer InSb/DKDP structure is bonded, on the crystal side, to a CaF substrate which has an expansion coefficient similar to that of DKDP. The two electrodes are connected to a programmable voltage source V_b as shown. Thermoelectric cells are bonded to the CaF substrate in the region outside the active area of the device, and the entire assembly is enclosed in a vacuum-tight chamber with write and readout windows. The actual vacuum demountable cell with its ethylene glycol chiller and sorption pump is shown in Figure 1a.

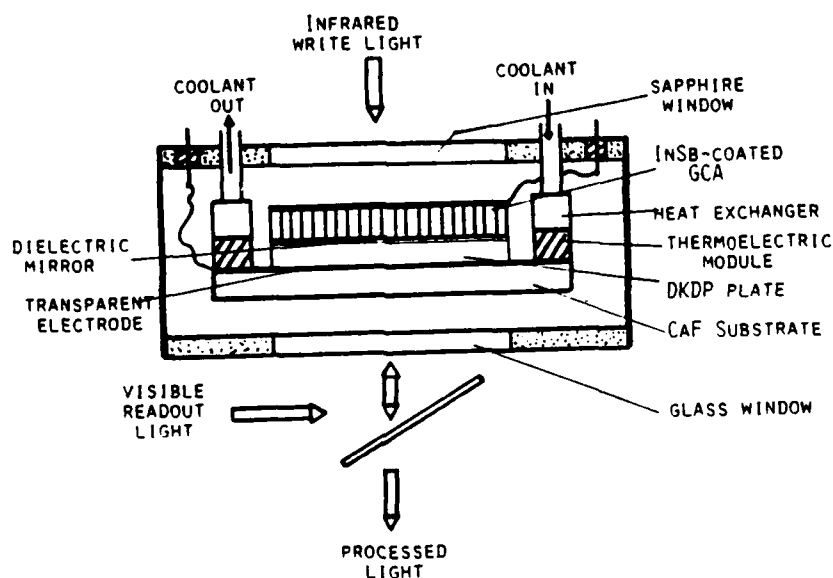


Figure 1a. Architecture of the InSb-DKDP Infrared-Sensitive Light Modulator

Figure 1b. Photograph of Vacuum-Demountable InSb/DKDP Modular Cell

The cell is evacuated with a liquid-nitrogen sorption pump and cooled near the Curie temperature of DKDP with five thermoelectric cells. The hot side of the thermoelectric modules are mounted to a liquid (ethylene glycol) cooled heat sink. The cooling procedure consist of two steps. The liquid cooling system reduces the temperature to 0°C , then the thermoelectric modules are turned on to cool the crystal/substrate to -51°C .

The major problem with this device design arises from the low dielectric strength, low resistivity and the concomitantly short discharge time constant of the InSb photoconductor. Furthermore, the resistivity of the InSb does change dramatically when exposed to light.

SECTION III

PRINCIPLES OF OPERATION OF THE DEVICE

Let us assume that the photodetector layer is ideal. That is, it exhibits low noise, high dark resistance (low leakage current), and intensity controlled resistance when illuminated in the 3-5 μm wavelength range. The device may be modelled as shown in Figure 2.

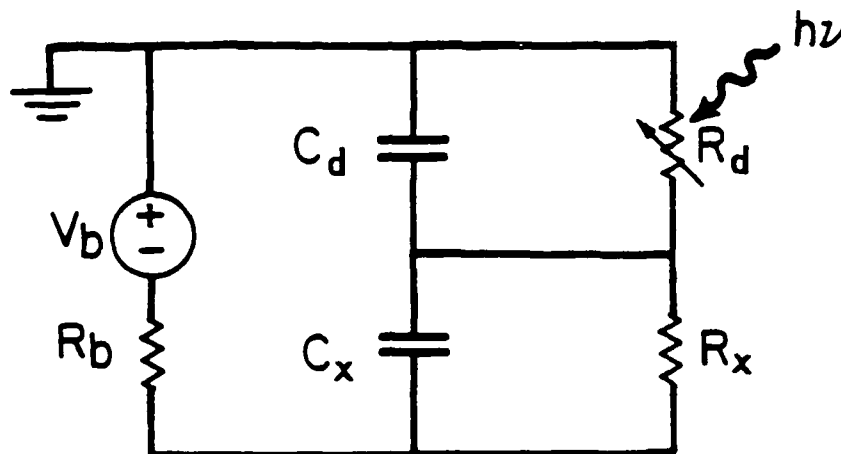


Fig. 2. Electrical Model of the Device

Thus, before the write light is turned on, the bias voltage V_b across the device will initially divide capacitively between the photodetector and the crystal such that

$$V_b = V_d + V_x \quad (1)$$

where

$$V_d = \frac{C_x}{C_x + C_d} V_b \quad (2)$$

and

$$V_x = \frac{C_d}{C_x + C_d} V_b \quad (3)$$

where V_d , C_d , V_x and C_x are the voltages and capacitances across the photoconductor and the crystal respectively.

When the write light is turned on, the photodetector is activated and charge

accumulates at the interface between the photodetector and the insulating light-blocking layer. This accumulated charge density σ_s changes the voltage V_x across the crystal to

$$V_x = \frac{\bar{C}_d V_b - \sigma_s}{C_x + C_d} \quad (4)$$

where \bar{C}_x and \bar{C}_d are the capacitances per unit area of the crystal and the photoconductor respectively. Hence, the change in the crystal voltage due to the illumination will be

$$\Delta V_x = \frac{\sigma_s}{C_x + C_d} \quad (5)$$

Since the crystal is electro-optic, the readout light, which makes a double-pass through the crystal is phase modulated according to its polarization. Thus, for z-cut DKDP, the image can readout with the aid of crossed polarizers. The light-induced halfwave voltage V_π is developed across the crystal when $\Delta V_x = V_\pi$. The corresponding halfwave exposure E_π is therefore given by

$$E_\pi = \frac{V_\pi}{S_d} (\bar{C}_x + \bar{C}_d) \text{ J/cm}^2 \quad (6)$$

where $S_d = J_d/I_w$ (amps/Watt) is the responsivity of the photodetector. Here J_d is the photocurrent density produced by the write light of intensity I_w . In order to minimize the halfwave exposure and the operating voltages, and to avoid dielectric breakdown in the photoconductor, it is highly desirable to make $C_d \ll C_x$ so that the full value of V_b that falls across the detector in dark can be transferred across the crystal as the device is exposed to the write light.

To erase the image, the charge distribution is removed from the interface by flooding the photoconductor with light and reversing the current flow in the photoconductor.

SECTION IV

ELECTRO-OPTIC MATERIALS CONSIDERATIONS

Liquid crystals, because of their relatively low operating voltages, would have been an attractive material for effecting light modulation in these devices. However, because of noise considerations, the detector material must be cooled and this precludes the use of common liquid crystals. DKDP when cooled near its Curie temperature offers a significant reduction of its halfwave voltage, and it is the material that was chosen for investigation. Another very attractive material, with perhaps a slightly smaller halfwave voltage, is DCDA (detuerated cesium dihydrogen arsenate).

ELECTRO-OPTIC EFFECT IN DKDP

Deuterated potassium dihydrogen phosphate, KH_2PO_4 (DKDP) is an uniaxial crystal. For our InSb/DKDP device, the propagation direction of the optical field is along the optical axis (z axis) of the crystal, and so the ordinary and extraordinary beams propagate with the same velocity such that there is no double refraction. When an electric field E_z is applied to the crystal, the birefringence is altered such that the allowed polarization directions of two components (x' and y') are rotated by 45° relative to the crystallographic x and y axes. When the crystal is operated in the reflex mode, for light polarized along either x' or y' , the change of the refractive index is

$$\Delta n = \pm n_0 r^3 E_z \quad (7)$$

where n is the refractive index of ordinary beam, and r is the element of the electro-optic tensor.⁸ If the applied voltage is V , the length of the crystal is L , then $E_z = V/L$. As a result the phase shift between the two polarization components of the output light is

$$\Gamma = \phi_{y'} - \phi_{x'} = \frac{4\pi n_0^3 r_{63} V}{\lambda} \quad (8)$$

where λ is the wavelength of readout light. When $\Gamma = \pi$, we find that the halfwave voltage V_π is given by

$$V_\pi = \frac{\lambda}{4n_0^3 r_{63}} \quad (9)$$

Hence,

$$\Gamma = \frac{V}{V_\pi} \pi \quad (10)$$

With the polarization vector of the incident readout light parallel to the x

axis, and an analyzer in the output plane with its polarization direction parallel to y axis, it can be shown that the output intensity of this system is given by

$$I_o = I_i \sin^2(\Gamma/2) \quad (11)$$

where I_i is the intensity of incident readout light. If a bias V_b is arranged so that it imparts a static retardation Γ_b equal to $\pi/2$, then when the write light is turned on, the transmittance of crystal becomes:

$$\begin{aligned} \frac{I_o}{I_i} &= \sin^2 \left(\frac{\pi}{4} + \frac{\pi \Delta V_x}{2V_\pi} \right) \\ &= \frac{1}{2} \left\{ 1 + \left(\sin \frac{\pi \sigma_s}{V_\pi (C_x + C_d)} \right) \right\} \end{aligned} \quad (12)$$

and if

$$\frac{\pi \sigma_s}{V_\pi (C_x + C_d)} \ll 1,$$

$$\frac{I_o}{I_i} = \frac{1}{2} \left(1 \pm \frac{\pi \sigma_s}{V_\pi (C_x + C_d)} \right) \quad (13)$$

Because σ is proportional to the exposure of the infrared write light, we obtain a positive visible image modulated by the write infrared pattern. Using this output visible coherent image, we can perform real-time infrared pattern processing.

Let us again consider our InSb/DKDP device. The write light is in the wavelength range of 3-5 μm and the readout is generated by a He-Ne laser ($\lambda = 6328 \text{ \AA}$). For z-cut DKDP operated in the reflex longitudinal mode, the halfwave voltage V_π is 125 V at -51°C for a readout wavelength of 633 nm. The longitudinal dielectric constant of DKDP is 650, and if we assume a crystal thickness of 150 μm , this leads to a crystal capacitance of 3.8 nF/cm². This is comparable to that of a 4 μm thick layer of InSb with a dielectric constant of 17.7. Thus, if we take $C_x = C_d$ and assume a write light wavelength of 4 μm and a quantum efficiency of 0.7, we find that the calculated exposure sensitivity E_p is approximately 2.8 $\mu\text{J}/\text{cm}^2$. From the foregoing, it is clear that V_b must be on the order of 200V to successfully operate such a device. This means that the InSb layer must withstand about 200 volts without breakdown. The fact that the device is cooled to -51°C and that the detector material can be amorphous favor an increased dielectric strength and discharge time constant over those of the single crystal material at room temperature.

SECTION V

PHOTOCONDUCTOR MATERIALS CONSIDERATIONS

PHYSICAL PROPERTIES OF INDIUM ANTIMONIDE (InSb)

As pointed out earlier, we have chosen InSb as the photoconductor for this device development effort. InSb is a narrow gap III-V semiconductor that crystallizes in a zinc blende structure. Indium is one sublattice and antimony is the other (see Figure 3) (Reference 8). The lattice constant, a , of the crystal is 6.47877\AA , making it the largest of the III-V zincblende structure compounds (Reference 10). Its physical properties are summarized in Table 1. InSb has the lowest melting point [798°K (525°C)] of all III-V zinc blende compounds (see Table 2). It is this low melting point that enables InSb to be recrystallized easily using zone melting methods. Its physical properties are summarized in Table 1.

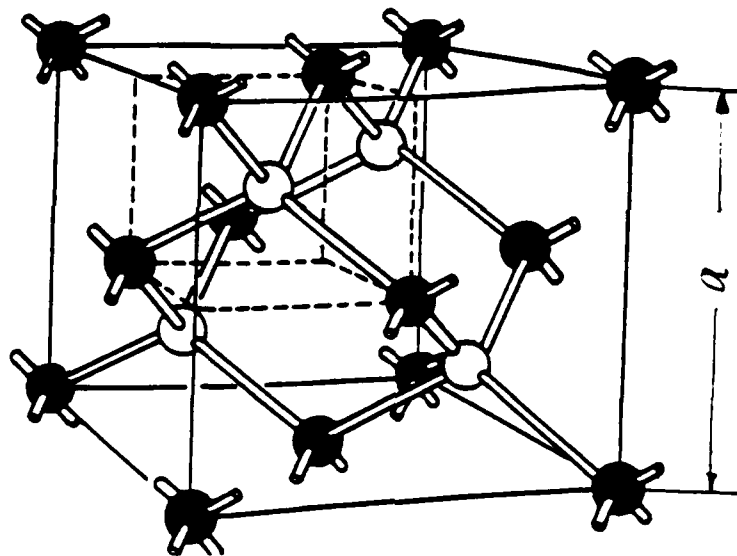


Figure 3. Cubic Unit Cell of the Zinc-Blende Structure Containing Eight Atoms

The bandgaps of most semiconductors increase as their doping and temperature decrease. The bandgap of InSb is 0.17 eV at room temperature and it increases by $2.8 \times 10^{-4}\text{ eV}$ for each degree centigrade decreased (Reference 9). The larger the bandgap, the more resistive the material, and hence the desire to operate the material at low temperature.

The material also has a very small effective mass for electrons at the bottom of the band, which implies that the band has a very high curvature at its minimum and a very low density of states there. As a result, a small number of electrons fill the band to a high level.

TABLE 1. PHYSICAL PROPERTIES OF InSb (Reference 9,10)

Crystal Structure:	zinc blende
Dark Resistivity:	1-2 Ω cm
Lattice Constant:	6.47877 Å
Electron Mobility:	10^5 cm ² /Vsec
Melting Point:	798° K (525° C)
Hole Mobility:	1700 cm ² /Vsec
Dielectric Constant:	17.7
Typical Minority:	10^{-8} - 10^{-9} sec
Carrier Lifetime:	for p-type
Refraction Index:	4.02 @ 4 μ m
Bandgap (300 K):	0.164 eV (direct)
$\Delta E_g/^{\circ}$ C:	-2.8×10^{-4} eV/ $^{\circ}$ C

Table 2. MELTING POINTS OF III-V COMPOUNDS (Ref. 10)

InSb	525.2 C	GaSb	712.2 C	AlSb	1050 C
InAs	942 C	GaAs	1273 C	AlAs	> 1600 C
InP	1062 C	GaP	1450-1500 C		

Table 3. PROPERTIES OF III-V COMPOUNDS AT ROOM TEMPERATURE (Ref. 10)

Material	Energy gap (ev)	Electron mobility (cm ² /Vsec)	Hole mobility (cm ² /Vsec)	m_e/m_0	m_h/m_0	Refractive index	Dielectric constant
InSb	0.17	78,000	750	0.013	0.6	3.96	17
InAs	0.36	33,000	460	0.02	0.4	3.42	14
InP	1.29	4600	150	0.07	0.4	3.26	14
GaSb	0.67	4000	1400	0.05	0.5	3.74	15
GaAs	1.39	8500	420	0.07	0.5	3.30	12.5
GaP	2.25	110	75			2.91	10
AlSb	1.62	200	420		0.4	3.18	11
Ge	0.66	4000	2000	0.22*	0.3	4.00	16.0
Si	1.09	1600	500	0.33*	0.5	3.44	11.8

* Density of states mass

PHOTOCONDUCTIVE PROPERTIES OF InSb

The photoconductive properties depend strongly on the mobility of the material, and on the size of the effective mass. In this regard, we can see from Table 3 that InSb offers several advantages over the other III-V compounds. It has high mobility and a small effective mass of conduction electrons. The hole mobility of InSb, μ_h , is 750 cm²/Vsec and the electron mobility, μ_e , is 78,000 cm²/Vsec at room temperature. Both mobilities are dependent on temperature. Above 200 °K, the mobilities are given by (Reference 10)

$$\mu_e = 7 \times 10^8 \times T^{-1.6} \text{ cm}^2/\text{Vsec} \quad (14)$$

$$\mu_h = 1.1 \times 10^8 \times T^{-2.1} \text{ cm}^2/\text{Vsec}$$

Figure 4 shows the temperature dependence of electron and hole mobility in InSb. The mobility of holes and electrons also determine the resistivity of the semiconductor via the relation:

$$\rho = \frac{1}{q(\mu_e N + \mu_h P)} \quad (15)$$

where q is the magnitude of electric charge and N , P are the electron and hole densities respectively.

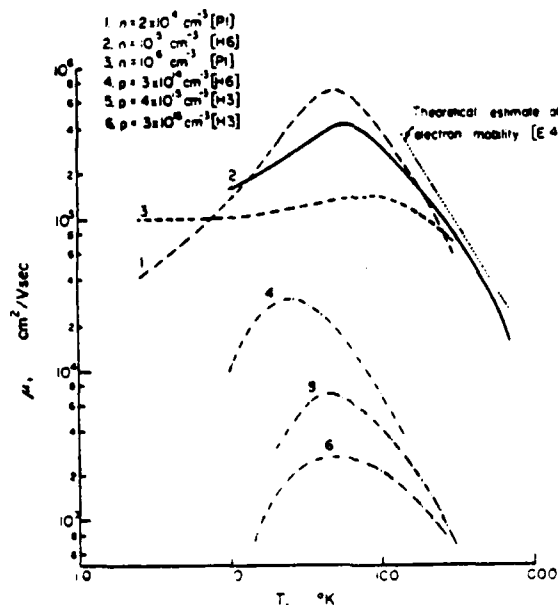


Figure 4. Temperature Dependence of Electron and Hole Mobility in InSb (Reference 10)

Diffusion length and diffusion lifetime are very important parameters in the studies of photoconductivity. Both lifetime and diffusion length depend on the temperature. Figure 5 shows the temperature dependence of minority and majority carrier lifetimes for p-type InSb. At 77°K, the carrier lifetimes are near 2×10^{-10} sec implying an improved photoconductive response at low temperature.

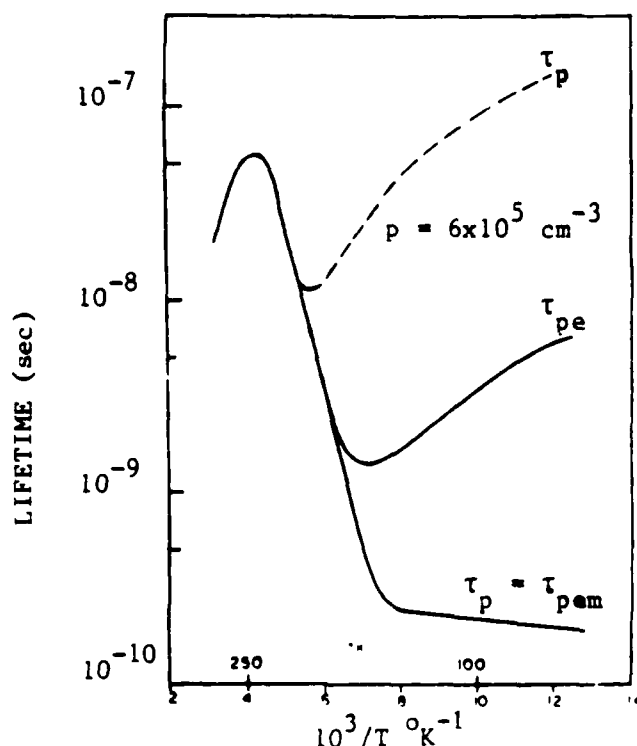


Figure 5. Temperature Dependence of Minority and Majority Carrier Lifetimes for P-Type InSb (Reference 10)

In this program, we investigated the photoconductivity of InSb films deposited on glass by flash evaporation. Figure 6 shows the room temperature spectral response of the photoconductive current (normalized to equal incident energies) of evaporated InSb films for the spectral range between 2 and 4.5 μm . Figure 7 shows typical spectral detectivity range for cooled photoconductive InSb of various areas; 2π FOV; 77K, 300K background.

Because InSb, like other III-V compounds, exhibits low dark resistivity, the modulator design employs this material in a discrete pixel array separated by insulating barriers (to prevent transverse migration of charge). Alternatively, it should be possible to employ a Schottky barrier type electrode on the write light side and deplete the semiconductor before operation as a detector.

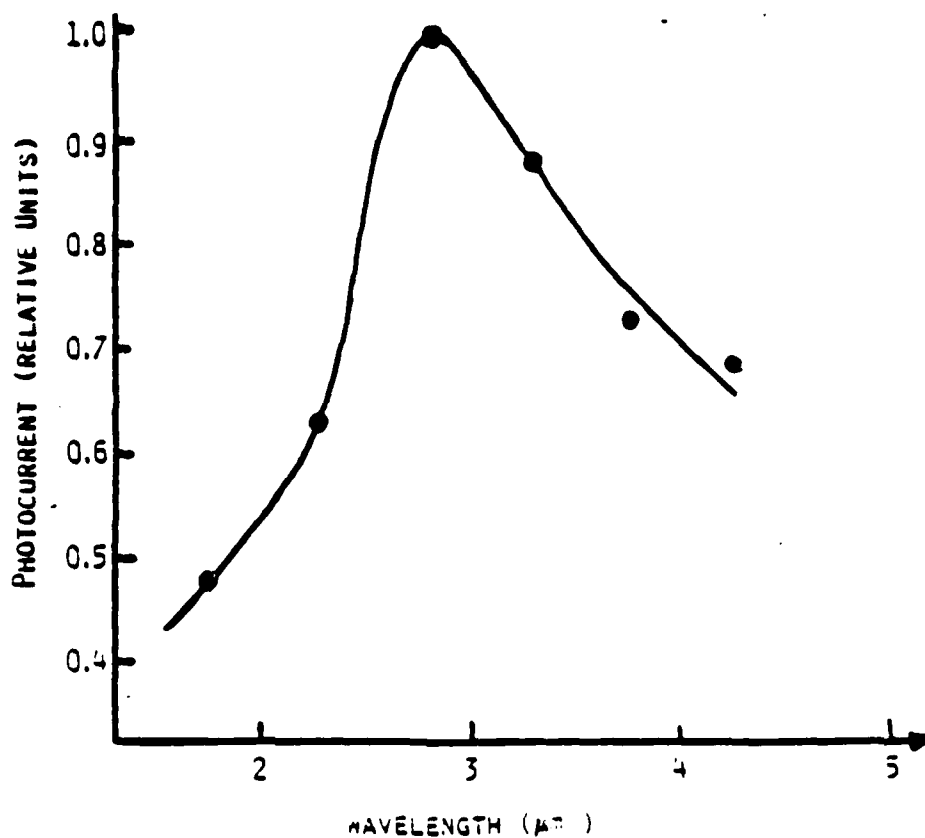


Figure 6. Photoconductivity of a Thin Flash Evaporated Film of InSb

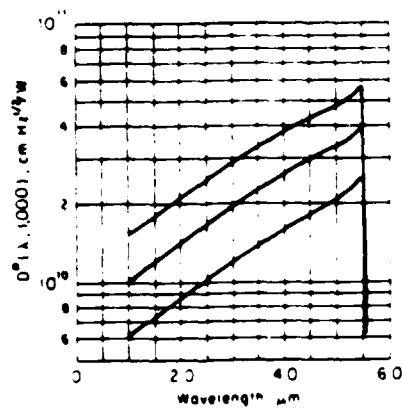


Figure 7. Typical Spectral Detectivity Range for Cooled Photoconductive InSb of Various Areas; 2π FOV; 77°K , 300°K Background

If we assume that the thickness t_p of the photoconductor is less than $1/\alpha$, the penetration depth of the write light, then under steady state illumination, the initial carrier generation rate is given by

$$G = \frac{n}{\tau} = \frac{\eta(I_w/h\nu)}{t_p} \text{ cm}^{-3}\text{sec}^{-1} \quad (16)$$

where τ is the carrier lifetime, n is the number of carriers per unit volume, I_w is the write light intensity, η is the quantum efficiency of the photogeneration process, h is Planck's constant, ν is the frequency of the write light.

The photocurrent density through the photoconductor is given by

$$J_p = \sigma E = q\mu_n E = qn\nu_d \quad (17)$$

where E is the electric field, σ is the conductivity of the photoconductor, q is the electronic charge, μ_n is the carrier mobility and ν_d is the drift velocity. Substituting for n , we find

$$J_p = \left(\frac{\tau}{t_p}\right) \frac{q\eta I_w}{h\nu} = S_p I_w \quad (18)$$

Where t_p is the carrier transit time and τ/t_p is the photoconductive gain.

This leads to a change in the interface surface charge density σ_s that is given by

$$\begin{aligned} \sigma_s &= \int_0^T J_p(t) dt \\ &= - \left(\frac{\tau}{t_p}\right) \frac{q\eta I_w T}{h\nu} \end{aligned} \quad (19)$$

if a constant voltage is maintained across the photoconductor by ramping V_b . As before, Equations (4) and (5) give the relationship between this surface charge distribution and the crystal voltage. If V_b is not ramped and the write light remains on, the device will charge until the voltage across the photoconductor falls approximately to zero and the crystal voltage rises to

approximately V_b . To erase the device, the photoconductor is flooded with light and V_b is reversed; the interface surface charge distribution then bleeds off through the photoconductor.

NOISE CONSIDERATIONS

The rms noise current density in a photoconductor is given by

$$J_n^2 = J_{gr}^2 + J_j^2 + J_{1/f}^2 \quad (20)$$

where J_{gr} is the generation-recombination (g-r) noise, J_j is the Johnson noise and $J_{1/f}$ is the 1/f noise. The g-r noise is inherent to the quantum detection process itself, and if the device is properly operated, it will be the dominant source of noise.

The thermal (Johnson) noise current density in a photoconductor is given by

$$J_j^2 = \frac{4kTR\Delta f}{A} = \frac{4kT\Delta f \rho \ell}{A^2} \quad (21)$$

where k is Boltzman's constant, Δf is the modulation bandwidth of the radiation, T is the temperature, R is the resistance, A the area of cross section, and ρ the resistivity of the photoconductor material. If we illuminate the photoconductor with modulated light of frequency ω such that

$$I_w(\omega) = I_0(1 + m \cos \omega t) \quad (22)$$

then the rms signal current density is given by

$$J_p = \frac{nqmf_0}{\sqrt{2h\nu}} \left(\frac{\tau}{t_r} \right) \frac{1}{(1 + \omega^2 t^2)^{1/2}} \quad (23)$$

and the generation-recombination shot noise by ^{8,9}

$$\bar{J}_{gr}^2 = \frac{\tau}{t_r} \frac{4qJ_0\Delta f/A}{1 + \omega^2\tau^2} \quad (24)$$

where J_0 is the steady-state light-induced current density. The foregoing equations lead to a signal-to-noise S/N ratio that is given by⁹

$$(S/N) = \frac{J_p^2}{\bar{J}_j^2 + \bar{J}_{gr}^2} = \frac{\eta m^2 A I_0}{8h\nu\Delta f} \left[1 + \frac{kT}{q} \frac{t_r}{\tau} (1 + \omega^2\tau^2) \frac{1}{R_{J_0}A} \right]^{-1} \quad (25)$$

Correspondingly, in a photodiode shot noise currents (due to the randomness of the hole electron generation process) arise because of the presence of background light, thermal generation in the depletion region (dark current) and because of the signal itself. The noise current density associated with these processes can be written as

$$\langle J_s^2 \rangle = 2q(J_B + J_{dk} + J_D)\Delta f \quad (26)$$

Thus, the signal-noise ratio for a photodiode with $m = 1$ is given by.⁹

$$(S/N) = \frac{1/2(q\eta I_0/h\nu)^2 A}{2q(J_B + J_{dk} + J_D)\Delta f + 4kT\Delta f/AR_{eff}} \quad (27)$$

where we have included the Johnson noise due to the effective reverse biased resistance of the device.

The minimum detectable write light intensity, I_{wmin} , or the noise equivalent intensity, NEI, is the optical power that corresponds to a $S/N = 1$, and this can be inferred from Equations (25) and (27).

For example, for a photoconductive device, Equation (25) shows that the shot-noise-limited (g-r noise) minimum detectable intensity is given by

$$I_{wmin} = \frac{8h\nu\Delta f}{\eta A} \text{ W/cm}^2 \quad (28)$$

For InSb with $\eta = 0.7$, taking $\lambda = 4 \mu\text{m}$, $A = 1/\text{cm}^2$, $\Delta f = 1 \text{ Hz}$, we find $I_{w\text{min}} = 5.6 \times 10^{-19} \text{ W/cm}^2$ for quantum-limited detection. And, in the case where the dominant noise is due to the background photon flux Q_B , it can be shown that the background-limited detectivity D_{blip} is given by¹³

$$D_{\text{blip}}^* = \frac{\lambda}{2hc} \sqrt{\frac{\eta}{Q_B}} \quad (\text{for a photoconductor}) \quad (29)$$

and

$$D_{\text{blip}}^* = \frac{\lambda}{hc} \sqrt{\frac{\eta}{2Q_B}} \quad (\text{for a photodiode}) \quad (30)$$

Since the device integrates charge at the detector-blocking layer interface, another important noise parameter is the maximum exposure time, which is the time it takes for the minimum detectable intensity plus the noise to accumulate an interface charge density that changes the crystal voltage by the halfwave voltage. Thus, using Equation (6), we can write

$$T_{\text{max}} = \frac{V_{\pi}(\bar{C}_x + C_d)}{2SI_{w, \text{min}}} \quad (31)$$

For a photoconductive modulator, the quantum-limited $T_{p, \text{max}}$ is, therefore, given by

$$T_{p, \text{max}} = \frac{V_{\pi}(\bar{C}_x + \bar{C}_d)}{16 \left(\frac{\tau}{t_r} \right) q \Delta f} \quad (32)$$

For our InSb modulator in the above example, this yields a maximum of exposure time of $9.5 \times 10^{10} \text{ sec}$.

FLASH EVAPORATION

Flash evaporation has been used to deposit binary and ternary or III-V intermetallic semiconductive films, (References 11-13). The salient features of our flash evaporation apparatus is shown in Figure 8a and the actual system is shown in Figure 8b. The procedure that we used for flash evaporation of the InSb was as follows. The InSb was first ground to a fine powder (100 mesh) and placed in the powder reservoir within the vacuum chamber [see Fig 8a]. The powder dispenser controls the rate at which the powder grains are fed to crucible, to which they are guided by the chute. After the chamber was pumped out to about 10^{-6} torr, the crucible was heated by the direct passage of a current through it (Joule heating) to a temperature ($\sim 1300^{\circ}\text{C}$) well above that required for the evaporation of the least volatile component of the source material. Each grain which drops onto the crucible dissociates and contributes a quantity of vapor whose composition changes continuously, starting with the most volatile group V element and terminating with the least volatile group III element. The rate of feed of the powder is adjusted so that at equilibrium the element components in the vapor are present in the stoichiometric ratio of the source compound. The substrate G (a microscope slide in these initial experiments) was heated by a resistive heater.

A metal plate (baffle) placed between the substrate and hot boat was used to prevent any deposition on the substrate before the system reached the proper pressure and temperature. The plate was swung aside just before the InSb powder was dropped into the hot boat. At the conclusion of the evaporation, the heaters of the boat and the substrate were turned off and the substrate left to cool in the vacuum for 2 to 4 hours. The crystallinity of the deposited films was found to be a strong function of the temperature of the substrate and the crucible.

A tungsten boat was used because of its very high melting point ($3410 \pm 20^{\circ}\text{C}$). The powder dispenser is actually a small buzzer that vibrates the powder reservoir. In order to control the rate of feeding powder, different hole sizes (gates) are selected at the output of the reservoir. This vibratory powder dispenser has the following advantages: the powder flow is not dependent on the amount of material in the powder reservoir; the gate is larger than the powder particles, thus the flow remains constant; the gate size can be easily changed to alter the feed rate of powder.

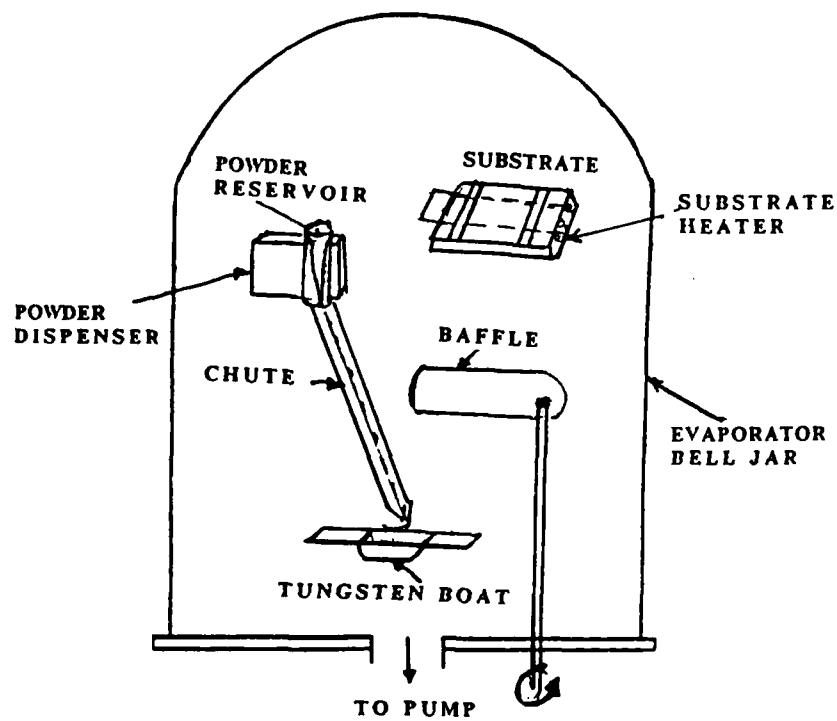


Figure 8a - Setup for Flash Evaporation of InSb

Fig. 8b - Actual Flash Evaporation System Used

CHARACTERIZING PHOTOCONDUCTIVITY RESPONSE OF InSb

The experimental setup for measuring the photoconductivity of the InSb films is shown in Figure 9. The Oriel 6361 infrared source housing consists of a 6363 IR element, a 6362 IR germanium condensing lens, a filter holder and a 6329 DC regulated power supply. The IR source with a 6x20 mm active area is installed in a black lamp housing. It provides continuous emission from 0.7 to 20 microns and operates up to a temperature of 1000K. Before the measurements were taken, the lamp was warmed up for 30 minutes. Figure 10a shows the intensity of the bare element per 10cm area from 0.7 to 28 microns. The germanium condensing lens has a usable transmission curve from 2.7 to 16 microns as shown in Figure 10b.

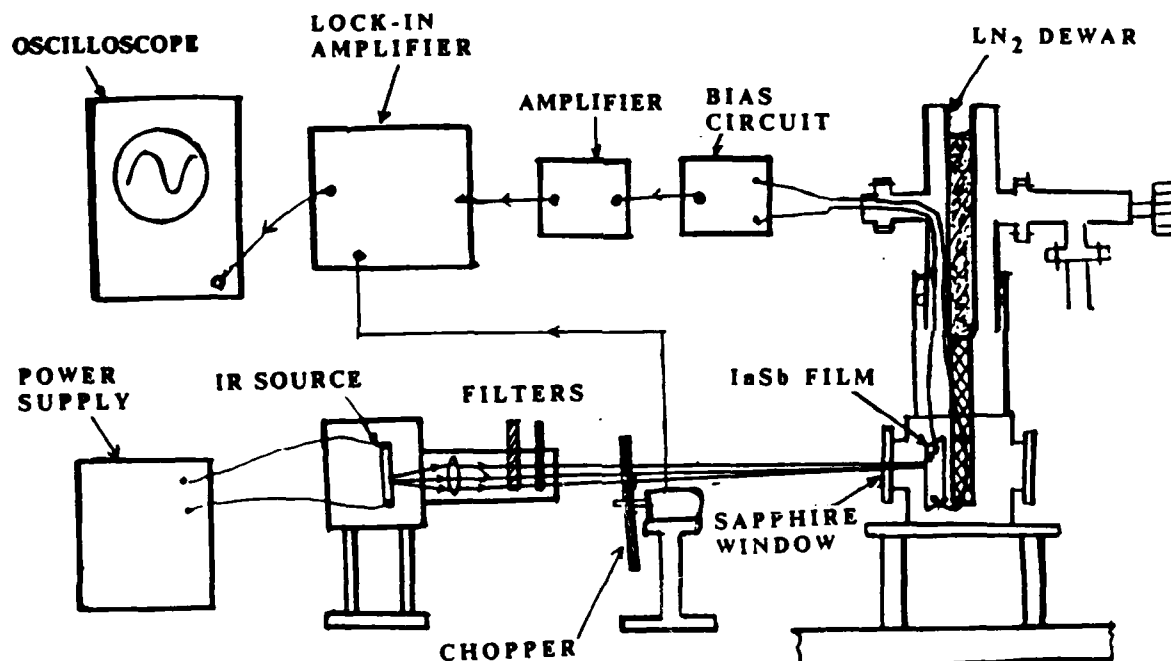


Figure 9. Experimental Setup for Measuring Photoconductivity of InSb Films

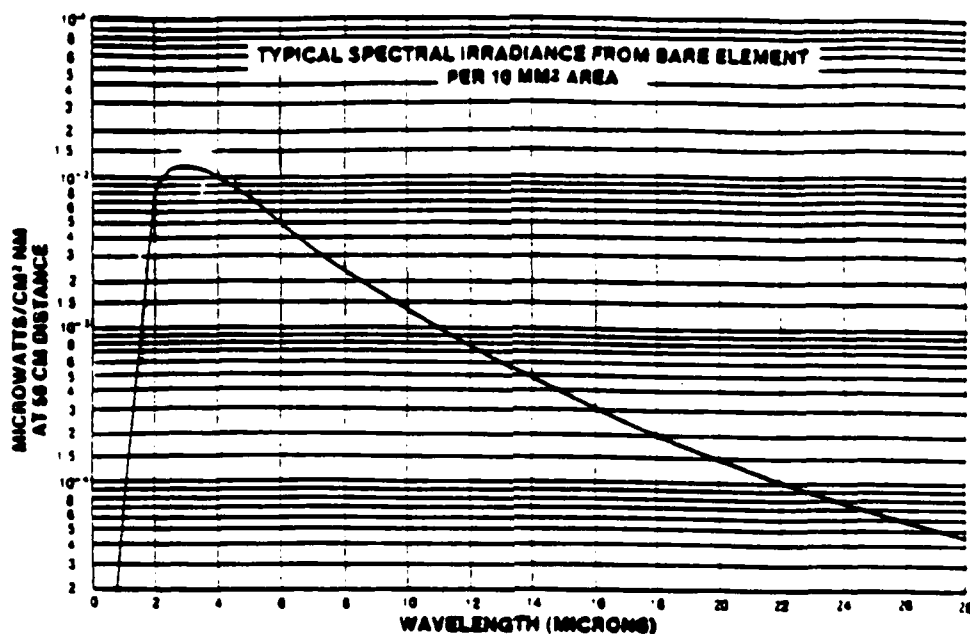


Figure 10a. Spectral Output of the Oriel Infrared Lamp Used
(Oriel Catalog)

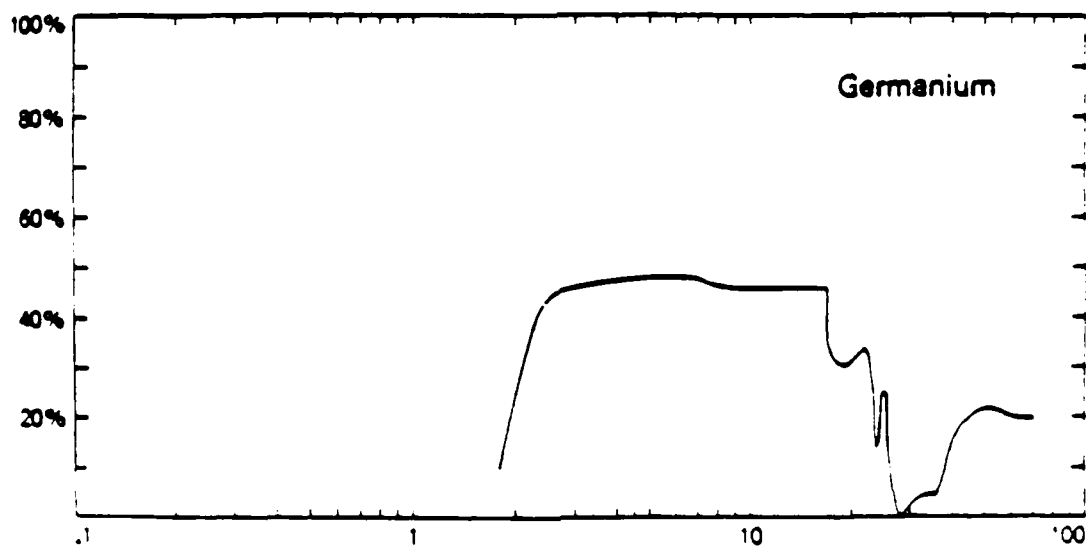


Figure 10b. Spectral Transmittance of the Germanium Lens
(Laser Focus Buyers Guide)

A filter holder was mounted at the end of the condensing lens assembly. The filter assembly used was actually a combination of a long pass filter and a short pass filter that effectively transmitted only a narrow band of radiation. The DC power supply was connected to the IR source to regulate the amount of voltage and current applied to the lamp. This power supply can generate 5 to 13 volts. In our experiments, the power supply was set at 11 volts and it drew 12 amperes of current.

A chopper with a frequency of 59.8 Hz was placed between the filters and the InSb sample. The InSb film was placed in contact with the cold finger of a liquid N₂ dewar and cooled down to 225K (-48 °C). Electrodes were mounted onto the thin film of InSb using "Epo-tek-H20E" silver epoxy. The radiation through the chopper fully covered the portion of InSb without silver paint. Measured currents varied from 20 mA to 200 mA. The signal V_c was amplified with an operational amplifier (gain of 500 - 1000) and processed by standard lockin amplifier techniques. Typical photoconductive results for our flash evaporated films are shown in Figure 6.

SECTION IV

CONCLUSIONS

During the 24-month duration of the technical effort, the tasks completed included:

The architectural design of the InSb/DKDP light modulator as illustrated in Figure 1; the fabrication and testing of the vacuum cell (with sapphire and glass windows and electrical feedthroughs) that houses the heat exchanger, Peltier coolers and the InSb/DKDP substrates; the fabrication and testing of the heat exchanger that removes heat from the Peltier cells to the exterior of the vacuum chamber; the assembly, installation and testing of an ethylene glycol recirculating cooler and heat exchanger; the mounting of a CaF substrate on the Peltier cells, and the testing of the cooling characteristics of the Peltier cells; the assembly and bonding of the Peltier coolers to the CaF substrate; the testing of the Peltier coolers to -40°C ; the cutting and crystal polishing of two DKDP crystals; the mounting of the DKDP crystal to the CaF substrate; the retesting of the cooling characteristics of the entire system to -38°C ; the theoretical development and modelling of the operating characteristics of the modulator (e.g., sensitivity, spatial resolution, storage time, framing speed and noise characteristics); the rebuilding and modification of a homemade evaporator for the flash evaporation of InSb the fabrication of a special system for heating the InSb substrates in vacuum; the flash evaporation of several InSb films of varying thicknesses and annealed at various temperatures; the setup of a liquid nitrogen cryostat fitted with sapphire windows and electrical feedthroughs for cooling the InSb substrates and measuring their photoconductivity; the setup of the infrared photoconductivity system consisting of glo-bar source, combinations of long and short pass filters, collimating lens, chopper, and lock in amplifier; and the measurement of the photoconductivity of InSb films as a function of temperature and evaporation conditions.

A preliminary design of a liquid oxygen light modulator cell that would operate in conjunction with an InSb photoconductor at 77°K was contemplated, a simple construction of a simple liquid oxygen light modulation cell was fabricated, and we began development of the theory of electric-field-induced molecular orientation and refractive index modulation in liquid oxygen.

REFERENCES

1. B. A. Horowitz and F. J. Corbett, "The PROM - Theory and Application for the Pockels Readout Optical Modulator", *Optical Engineering* 17, 353-364, 1978
2. W. P. Bleha, et al, "Application of the Liquid Crystal Light Valve to Real-Time Optical Data Processing", *Optical Engineering*, 371-384, 1978
3. C. Warde, A. M. Weiss, A. D. Fisher, and J. I. Thackara, "Optical Information Processing Characteristics of the Microchannel Spatial Light Modulator", *Applied Optics*, 20, 2066-2074, 1981
4. C. Warde, And J. I. Thackara, "Oblique-cut LiNbO_3 Microchannel Spatial Light Modulator", *Optics Letters*, 344-346, 1982.
5. C. Warde and J. I. Thackara, "Operating Modes of the Microchannel Spatial Light Modulator", *Optical Engineering*, 695-702, 1982.
6. I. N. Kompanets, A. V. Parfenov, and Yu M. Popov, "Spatial Modulation of a Liquid Crystal and an Insulated Gallium Arsenide Crystal", *Sov. J. Quantum Electron*, 1070-1071, 1979
7. A. V. Parfenov, I. N. Kompanets and Yu M. Popov, "Spatial Modulation of Light in Photosensitive High-Resolution Metal-Insulator-Semiconductor Structures with Liquid Crystals", *Sov. J. Quantum Electron*, 1, 167-171, 1980.
8. S. M. Sze, Physics of Semiconductor Devices, Second Edition, John Wiley & Sons, New York, 1981
9. CRC Handbook of chemistry and physics, 61st ed, (1980-81)
10. C. Hilsum, A.C. Rose-Innes, "Semiconducting III-V lcompounds," Volume 1, International series of Monographs on Semiconductors, (1961)
11. M. M. Wieder, "Intermetallic Semiconducting Films," Volume 10, International Series of monographs in Semiconductors, (1970)
12. S. A. Semiletov, P. S. Agalarzade, and F. M. Kortukova, "optical properties of polycrystalline InSb Films," *J. Appl. Phys.*, 252 (1964)
13. C. Juhez and J. C. Anderson, "Electrical properties of Flash-evaporated epitaxial Insb Films, "Physics letters 12(3), (1964)

END

DATE

FILMED

5-88

DTIC